A NEW BAYESIAN SOURCE SEPARATION APPROACH TO BLIND DECORRELATION OF SAR DATA

Alexander Wong and Paul Fieguth

Systems Design Engineering
University of Waterloo

1. INTRODUCTION

The use of synthetic aperture radar (SAR) has become an integral part of terrestrial and environmental monitoring applications, such as sea-ice monitoring [1] and land cover classification [2]. In SAR imaging systems, electromagnetic pulses in the microwave range (e.g., C-band for RADARSAT-1) are transmitted towards the surface of the Earth. The amplitude and phase signals at the receiver are then combined as if they were produced from a much larger antenna than the one used to transmit and detect the pulses, thus creating a large synthetic aperture.

An important challenge faced in SAR imaging is the presence of speckle, which arises from the constructive and destructive interference of the backscatter signal. Such complex speckle patterns occlude important details, thus limiting the level of accuracy that can be achieved when analyzing such data. While a large number of new despeckling algorithms have been proposed [3, 4, 5], the performance of such methods are often limited due to the fact that a majority of such methods do not account for the coherence between backscatter signals, resulting in correlated speckle patterns. Therefore, an important step in SAR data reconstruction may be the decorrelation of the SAR data, which can then be processed using existing despeckling algorithms to greater effect. Such decorrelation is often difficult since the point-spread function (PSF) of the SAR imaging system is not readily available.

In this paper, we investigate a new Bayesian source separation approach to blind decorrelation of SAR data, where the PSF is estimated directly from the SAR data. The key contribution is the patch-wise computation of the PSF, to account for spatial nonstationarities. Interestingly, similar nonstationary PSFs are present in medical ultrasound data, and this method should have similar applicability there.

2. METHODOLOGY

Assuming linear wave propagation and weak scattering, the received signal f is modeled as the convolution

$$f(x,y) = \int\int h(x,y,\alpha,\beta) \cdot r\,(\alpha,\beta)\,d\alpha d\beta + m(d,\theta), \tag{1}$$

where h is the PSF of the imaging system, m is all phenomena not accounted for by h, and r is the reflectance function defining the population of scatterers. While h is not spatially invariant, to simplify the model, h is commonly assumed to be spatially invariant within a sufficiently small region. As such, a segment from f, denoted as f', can

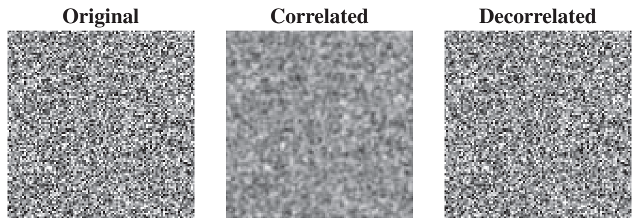

Fig. 1. Decorrelation results using simulated speckle

be modeled as the convolution of a linear, space-invariant PSF h' and a segment of the reflectance function r':

$$f'(x,y) = h'(d,\theta) * r'(x,y) + m(x,y), \tag{2}$$

Based on f', the demodulated, in-phase/quadrature data g' can be expressed as

$$g'(x,y) = f'(x,y) + j\mathrm{C}\left(f'(x,y)\right), \tag{3}$$

where C denotes the Hilbert transform. To decorrelate f', we must first estimate h'. Given the linear nature of the demodulation step, f' can be computed by taking the real part of g'. The Fourier transform of (2) is then

$$F'(u,v) = H'(u,v)R'(u,v) + M(u,v). \tag{4}$$

where H', R', and M are the Fourier transforms of h', r', and m, respectively. Assuming that the phenomena not accounted for by h' have little effect on the system, we simplify (4) by ignoring M, we can decouple H' and R' by performing the logarithm transform on (4):

$$\log\{|F'(u,v)|\} = \log\{|H'(u,v)|\} + \log\{|R'(u,v)|\}. \tag{5}$$

Given (5), the problem of estimating H' becomes an additive source separation problem, where the goal is to separate $\log\{|H'(u,v)|\}$ from $\log\{|R'(u,v)|\}$. We model the problem as Bayesian least squares

$$\hat{H}'_l(u,v) = \underset{H'_l(u,v)}{\arg\min}\left\{E\left[\left(H'_l(u,v) - \hat{H}'_l(u,v)\right)^2 |F'_l(u,v)\right]\right\}, \tag{6}$$

where $H'_l(u,v) = \log\{|H'(u,v)|\}$ and $F'_l(u,v) = \log\{|F'(u,v)|\}$. From (6), the analytical solution is well known to be $\hat{H}'_l(u,v) = E\left[H'_l(u,v)|F'_l(u,v)\right]$. If we follow the common assumption that the prior $p(H'_l(u,v))$ is uniform in the situation where no prior information is known, the Bayesian estimator can be simplified to be a function of the likelihood $p(F'_l(u,v)|H'_l(u,v))$. Based on the common Gaussian scatter model for R', R'_l follows a Fisher-Tippett distribution [6]. Therefore, the likelihood $p(F'_l(u,v)|H'_l(u,v))$ can be expressed as

$$p(F'_l|H'_l) = 2\exp\left[2\left(F'_l(u,v) - H'_l(u,v)\right) - \ln 2\sigma^2_{F'_l} - \exp\left[2\left(F'_l(u,v) - H'_l(u,v)\right) - \ln 2\sigma^2_{F'_l}\right]\right]. \tag{7}$$

After estimating $\hat{H}'_l$, H' can be computed by taking the exponential transform and, finally, the SAR data F' can be decorrelated using the Wiener filter.

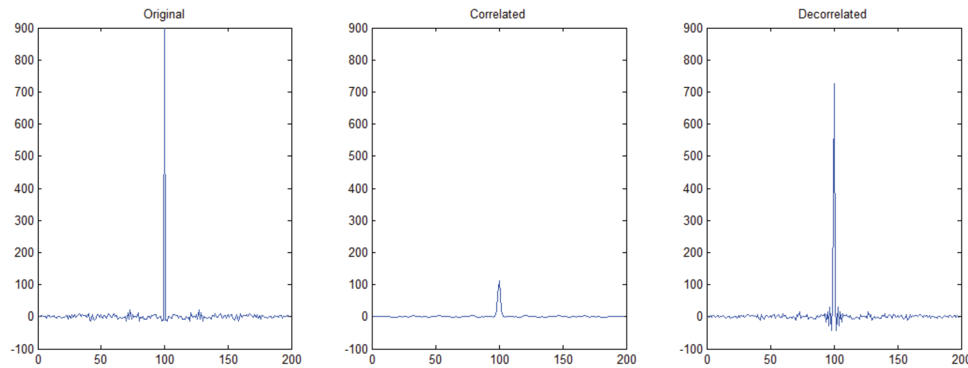

Fig. 2. Autocorrelation functions based on simulated data.

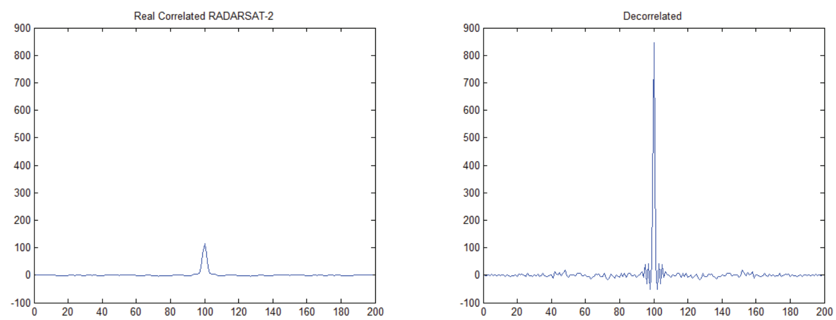

Fig. 3. Autocorrelation functions based on real, correlated RADARSAT-2 SAR sea-ice data.

3. EXPERIMENTAL RESULTS

To validate the proposed decorrelation methodology, we investigate its performance using both simulated SAR data and real RADARSAT-2 SAR sea-ice data obtained from the Canadian Ice Service (CIS).

Figures 2 and 3 show the effect of the proposed decorrelation. That the simulated tests involve realistic assumptions is supported by the similarity in behaviour of the decorrelation in both simulated and real cases. The actual decorrelation of a small synthetic data patch was shown in Figure 1. At least for that one example, the ability to learn the correct PSF, to successfully decorrelate the patch, is clear.

The most impressive results are shown in Figure 4, where the method is applied to a large (1041×1041) sea-ice SAR image. The method is applied patch-wise, to take into account the spatial nonstationarities present in SAR. The sharpness of the decorrelated and despeckled image is striking, and would lead to improved classification, particularly in the small, elongated bright and dark morphological features.

Given the promising results obtained, future work involves applying the method to additional samples of SAR data, and then coupled with tests on classification algorithms, to test the efficacy of the decorrelation approach in improving SAR image analysis. Related tests will be performed on medical ultrasound images, which suffer from more striking nonstationarities than SAR, and frequently also with much inferior signal-to-noise ratios, where a decorrelative approach would have much to offer.

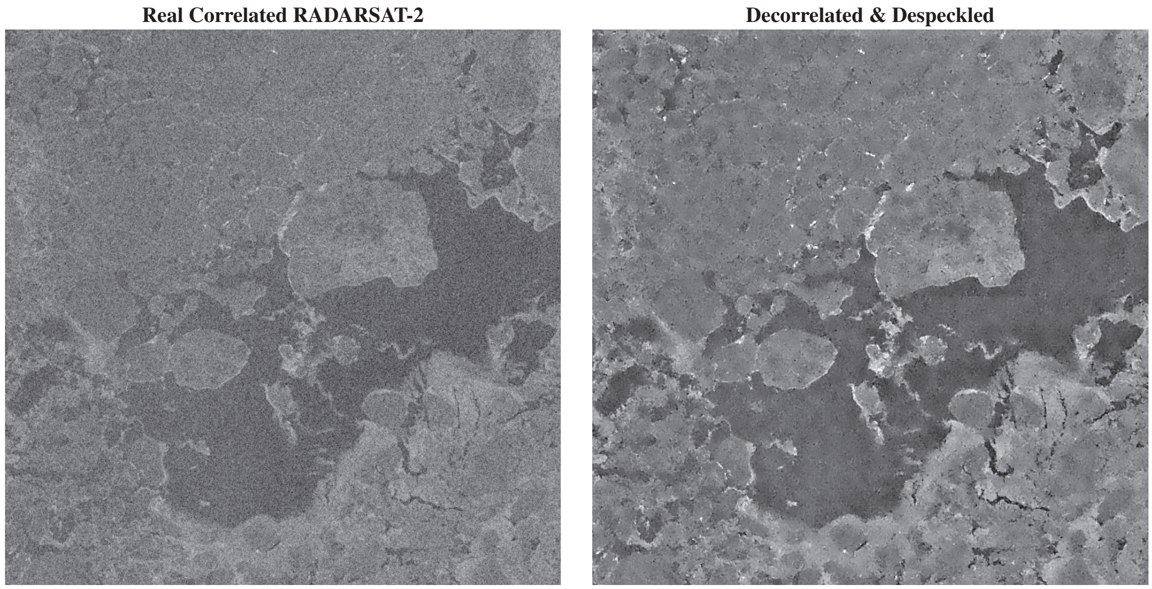

Fig. 4. Decorrelation results using an example RADARSAT-2 SAR sea-ice scene

Acknowledgment: We thank the Canadian Ice Service (CIS) for providing the RADARSAT-2 SAR sea-ice data.

4. REFERENCES

[1] Q. Yu and D. Clausi, "SAR sea-ice image analysis based on iterative region growing using semantics," *IEEE Transactions on Geoscience and Remote Sensing*, vol. 45, no. 12, pp. 3919-3931, 2007.

[2] C. Freitas, L. Soler, S. Sant'Anna, L. Dutra, J. dos Santos, J. Mura, and A. Correia, "Land Use and Land Cover Mapping in the Brazilian Amazon Using Polarimetric Airborne P-Band SAR Data," *IEEE Transactions on Geoscience and Remote Sensing*, vol. 46, no. 10, pp. 2956-2970, 2008.

[3] W. Zhang, A. Wong, and D. Clausi, "JEDI: Adaptive Stochastic Estimation for Joint Enhancement and Despeckling of Images for SAR," *Proc. 2009 Canadian Conference on Computer and Robot Vision*, pp.101-107, 2009.

[4] Y. Yu and S. T. Acton, Speckle reducing anisotropic diffusion, IEEE Trans. Image Process., vol. 11, no. 11, pp. 12601270, Nov. 2002.

[5] D. Gleich and M. Datcu, "Wavelet-Based Despeckling of SAR Images Using GaussMarkov Random Fields", *IEEE Transactions on Geoscience and Remote Sensing,* vol. 45, no. 12, part 2, pp. 4127-4143, 2007.

[6] H. Arsenault and G. April, "Properties of speckle integrated with a finite aperture and logarithmically transformed," *J. Opt. Soc. Amer.*, vol. 66, pp. 1160-1163, 1976.